

## Re-examine Re-examine deriving Oort constants from observational data

SHUFAN XIA,<sup>1</sup> KARENS MASTERS,<sup>1</sup> AND ZHAOYU LI<sup>2</sup>

<sup>1</sup>*Haverford College, Department of Physics and Astronomy*

<sup>2</sup>*Shanghai Jiaotong University, Department of Astronomy*

### ABSTRACT

The Oort constants parameterize stellar motion in radial, longitudinal, and latitude directions near the Sun. They can be used to find local galactic parameters, such as orbit ellipticity, solar distance from the Milky Way center and etc.. Further, they are closely related to the MW rotation curve. An accurate determination of this set of constants helps us derive the Milky Way rotation curve in the Sun's immediate neighborhood. *Gaia* provides massive and exquisite data on parallax and proper motion of stars in the Milky Way. These data make it possible to determine the Oort constants in the solar vicinity with unprecedented accuracy. This work re-examines the sampling limits on parallax and latitude in the Galactic coordinate for deriving the Oort constants based on observation data. We apply proper motion and line-of-sight velocity data from *Gaia* DR2 and compare the result with a 3D toy model simulation with test particles under axisymmetric potential to determine the best stellar subsets for calculating the Oort constants.

### 1. INTRODUCTION

The simplest model of the Milky Way(MW) will say our galaxy is a flat circular disk, and stars move on perfectly circular orbits around the galactic center. However, the structure and the dynamics of our galaxy is much more complicated. Our galaxy is a barred- spiral galaxy with non-axisymmetric and time-dependent perturbation to the potential. Furthermore, all stars have attained a random component to their orbital energy their orbits, so they move with deviations from perfect circular orbits (Binney & Merrifield 1998; Bovy 2017). The rotational kinematics of ME is complicated to quantify. The Oort constants are a set of empirically derived kinematic parameters  $A$ ,  $B$ ,  $C$ , and  $K$  that characterizes the local rotation properties in the Milky Way. It has been used extensively in the study of the rotational kinematics of our galaxy, and specifically, the galaxy rotation curve.

### 1.1. The Milky Way Rotation Curve

The measurements of the rotation curves of galaxies, a function of rotational velocity about the galactic center over distance, has led to the idea of dark matter's existence. From the flat but slightly rising rotation curve of the Milky Way (Fig.1), we came to our current understanding of the mass components and their distribution in our Galaxy.

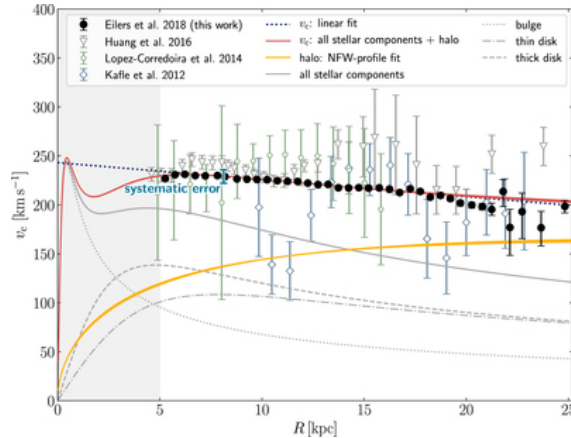


**Figure 1.** Historical measurements of the circular velocity curve of the Milky Way (Eilers et al. 2019).

With Newtonian Mechanics, we can connect velocity, potential, and mass distribution (Binney & Merrifield 1998); therefore, kinematics can serve as a mass detector. The implications of the rotation curve are multiple: it can be used to study kinematics, evolutionary histories of galaxies, and departures from Keplerian form due to dark matter (Sofue & Rubin 2001). However, measuring the Milky Way rotation curve is challenging because of the observation constraints from our location in the Milky Way. We are relatively close to the Galactic center and in one of the major spiral arms of the Galaxy (Binney & Merrifield 1998). This means that our line of sight is blocked by dust, so we can not observe the other side of the Galaxy. The fact that we are in the Galaxy and moving with it also makes it challenging to determine relative motion. Even with space telescopes, to make Milky Way measurement from outside the spiral arms or the Milky Way is. Therefore, measuring the whole rotation curve remains a daunting task.

Various objects and methods have been used to track the rotation curve. For the inner region within the sun, the MW rotation curve has been inferred via the tangent-point method using the line of sight velocity of H I or CO emission line measured from Doppler's effect Levine et al. (2008). The rotation curve of the outer region beyond the Sun has been measured by other tracers, such as classical Cepheid (Joy 1939; Metzger et al. 1998; Mróz et al. (2019)), RR lyrae variable Wegg et al. 2019, and luminous red giant stars Eilers et al. 2019.

### 1.2. Motivation



and  $190^\circ$  longitude, and minima at  $100^\circ$  and  $280^\circ$ . In Oort's original measurement, he looked at the data of a range of different types of stars and determined that near the Sun  $A \approx 19$  and  $B \approx 24(kms1kpc1)$ .  $A$  describes the local shearing, and  $B$  describes local vorticity. The result of a non-zero  $A$  provided the first strong evidence that the Milky Way is rotating differentially.

Later on, this analysis was generalized to consider the Sun's peculiar motion with respect to nearby stars. It is derived analytically that the double sin (or cos) trend is distinguishable from the pattern due to the Sun's peculiar motion about nearby stars. And two additional constants were introduced to the function of radial and tangential velocity against  $l$ ,  $C$ , and  $K$  (Ogrodnikoff 1932). These four constants,  $A$ ,  $B$ ,  $C$ , and  $K$  describe transverse shear, vorticity, radial shear, and divergence in the local velocity field from Galactic rotation accordingly. The radial velocity,  $v_{los}$ , is:

$$v_{los} = d(K + C\cos 2l + A\sin 2l) \quad (1)$$

The proper motion in longitude and latitude direction,  $\mu_l$  and  $\mu_b$ , have the following dependence on  $2l$  (Olling & Dehnen 2003):

$$\mu_l = (A\cos 2l - C\sin 2l + B)\cos b + \varpi(u_0\sin l - v_0\cos l) \quad (2)$$

$$\mu_b = -(A\sin 2l + C\cos 2l + K)\sin b \cos b + \varpi[(u_0\cos l + v_0\sin l)\sin b - w_0\cos b]. \quad (3)$$

In equations above, the single  $\sin$  and  $\cos$  terms represent the effect due to the sun's peculiar motion.

The Local slope of the rotation curve,  $\frac{d\Theta}{dr}|_{R_\odot}$ , is given by  $-(A + B)$ , and rotational velocity,  $\Theta_\odot$  is  $R_\odot(A - B)$ . If the galaxy is not axis-symmetric,  $C$  and  $K$  are nonzero (Binney & Merrifield 1998, Ogrodnikoff 1932). In the Method section, I (will) present the full derivation of Oort constants. The Fourier series approach has also been used to derive Oort constants. The Fourier coefficients in the 0 and 2 modes of the Fourier series approximation of proper motion in transceiver direction and angular velocity correspond to Oort Constants (Lin et al. 1978).

#### 1.4. Oort constants is localized

It must be emphasized that Oort constants can be extended to a set of functions depending on the distances from the Galactic center as we expand velocity fields about different distances. Typically, the Oort functions vary at a rate of a few  $km/s/kpc^2$  (Olling & Merrifield 1998). For distant stars in the disk, a higher order of the streaming velocity field equation must be taken into consideration (Siebert et al. 2011). The Oort constants in the first order of the streaming velocity field equation can only be used to restrain the Galactic rotation in the solar vicinity because the higher-order contributions will become significant at large distances (Bovy 2017). Due to the contribution from interstellar gas in the Milky which density varied non-monotonically with distance from the Galactic center, between  $0.9R_\odot$  and  $1.2R_\odot$ , the Oort functions  $A(R)$  and  $B(R)$  differ significantly from the general angular frequency dependence

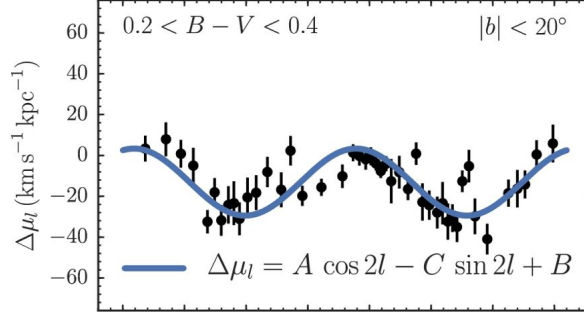


**Figure 3.** One example of historical measurement of Oort constants with observed proper motion in Galactic longitude: the value on  $y$ -axis is corrected for the solar motion based on Eq.3. The averages  $\mu_l(l)$  binned by  $l$  and their errors are plotted (Bovy 2017).

(Olling & Merrifield 1998). This suggests that when measuring the Oort constants, it is crucial to constrain the range of galactic distance.

### 1.5. Measure Oort constants from proper motion

Many investigations have been conducted to attempt to use proper motion to determine the character of the non-uniformity of rotation and to measure the Oort constants. Fig.3 shows one example of historical measurement of Oort constants with proper motion. However, not all the results are in agreement (Table 5, Kerr & Lynden-Bell 1986), which is mainly due to the absence of a complete proper motions catalog. A complete measurement of proper motion can give us stars distant enough that their random motions do not dominate their proper motions. It will also ensure sufficient sky coverage to allow the separation between the double sine curve of galactic proper motions from the single sine curve due to the solar motion in Eq.3 (Kerr & Lynden-Bell 1986). Although the observational precisions have been continuously developed, the values of  $A$  and  $B$  are still consistent with the values within uncertainties. However, for the values of  $C$  and  $K$ , it is another story (Li et al. (2019)). Besides needing a complete proper motion catalog, another three sources complicate an accurate determination of values for the Oort constants. First, the effect of non-axisymmetric potential associated with spiral or bar structure is not taken into account in Oort's analysis. Observation data suggests the necessity of looking at a non-axisymmetric mode (Metzger et al. 1998). From the radial velocity of Cepheid, a significant zero-point offset (Oort constant  $K$ ) in the radial velocities is suggested for a non-axisymmetric model. Metzger et al. 1998 also found a positive antisymmetric ellipticity component at R0. The deviations from the general axisymmetric velocity field to study the non-circular motions in great detail and infer the mass associated with the spiral arms. (Olling & Merrifield 1998)

Second, systematic errors due to the presence of spiral structure are likely to affect the measurements of the Oort constants. Moderate strength spiral structure causes errors of order  $5 \text{ km/s/kpc}$  in  $A$  and  $B$  (Minchev & Quillen 2007). The spiral structure can be understood in the light of density waves where the spirals have concentrated

stars. The streaming motion caused by density waves depending on the local spiral structure is difficult to determine (Lin et al. 1978). Further, the spiral structure raises the level of random motions in the Galactic disk (Sellwood & Carlberg 2014). Determination of other structural parameters to account for the effects from the Milky Way spirals must be made after a basic circular model.

Third, the nonuniform distribution of parallax over longitudinal in conjunction with the solar peculiar motion contributes to significant 0 and 2 order terms deviated from the first order Oort analysis (Olling & Dehnen 2003). This distribution of  $x(l)$  may be due to intrinsic density nonuniformity and observational errors due to interstellar extinction. The components due to this systematic error in the longitudinal proper motions  $\mu_l(l)$  are indistinguishable from the effect of double *sin* and *cos* dependency. The authors in Olling & Dehnen 2003 suggested using the latitudinal proper motions  $\mu_b(l)$  of stars at low latitudes could correct for the errors from mode mixing.

### 1.6. *Gaia* and Oort constants measurements

In previous decades, the HIPPARCOS telescope had been used extensively in studying the MW kinematics, including deriving local Oort Constants and the rotation curve from classical cepheid (Feast & Whitelock 1997, Mignard 2000, Olling & Dehnen 2003). The *Gaia* mission (Gaia Collaboration et al. 2016a), since its launch by the European Space Agency in 2013, has collected astrometric parameters with unprecedented accuracy and multitude, aiming to build a three-dimensional map of our Galaxy. By the second release of *Gaia* data, we have the parallax and proper motions of over 1,600,000,000 stars by its second release (Andrae et al. 2018). This also includes stars in higher latitude with significant latitude proper motion. Therefore, this large set of astrometric measurements allows the first truly local precise measurement of the Oort constant and investigation of fine local kinematic features.

Two studies of using *Gaia* DR1 and DR2 to calculate the Oorts Constant in solar vicinity yielded results in agreement (Bovy 2017; Li et al. 2019). The current values of the Oort constants based on DR2 is  $A = 15.1 \pm 0.1$ ,  $B = B = 13.4 \pm 0.1$ ,  $C = 2.7 \pm 0.1$ ,  $K = 1.7 \pm 0.2$ . The slope of the rotation curve is determined from  $-(A+B)$  is negative, thus confirming a slightly declining rotational curve in the solar vicinity. And significant non-zero C and K further indicate non-axisymmetric potential (Bovy 2017; Li et al. 2019). This suggests applying the axis-symmetric assumption of Oort analysis should be carefully examined. Both studies found the local Oort constants varied among different stellar populations based on their positions in the Hertzsprung-Russell Diagram. The result in Li et al. 2019 shows the red giants deviate from the main-sequence stars in all four constants because they show more elliptical orbits and larger velocity dispersion. This finding is inconsistent with the suggestion in Olling & Dehnen 2003 that red giants are the “true” tracer Oort constants because they are old enough to be in equilibrium and distant enough to be unaffected by possible



local anomalies. This disagreement suggests establishing an appropriate set of stars is critical to determine Oort constants accurately.

Previous two work of using HIPPARCOS or *data* to fit Oort constants used average proper motion binned by  $l$ , but fine features from each sample point in  $l$  vs proper motion are neglected (Bovy 2017, Li et al. 2019). Neither work used radial velocity information to determine the local Oort constants because the radial velocity is measured from not enough samples. However, a closer look at the radial velocity results and their deviation from the predicted theoretical model potentially entails significant information.

### 1.7. Proposed research

This work looks at the Main Sequence and red giant stars from *Gaia* DR2 and uses their latitudinal and longitudinal proper motions, and their radial velocity to determine the solar local Oort constants to higher precision. Each Individual sample is also considered in deriving Oort constants from proper motions.

As to measure Oort constants to higher precision, this works re-examine the conventional constraints on data sampling. In previous measurements of Oort constants (Olling & Dehnen 2003; Bovy 2017; Li et al. 2019), the sampling limit on parallax and latitude were explained qualitatively without much justification and ununified. For example, Olling & Dehnen 2003 suggested, using the  $\mu_b$  of low latitudes stars, but both Bovy (2017) and Li et al. (2019) adopted the  $40^\circ < |b| < 50^\circ$  sampling criteria. The importance of these limitations is to ensure the circular assumption of Oort constants is appropriate.

I uses a simple 3D toy model under circular orbital motion assumption to obtain a theoretical prediction of longitudinal and latitudinal proper motion,  $\mu_l$  and  $\mu_b$ , and radial velocity  $v_{los}$  as functions of Galactic longitude. The goal of this model simulation and comparing it to observational data is twofold. One, this simple model allows us to find the range of parallax and Galactic latitude that give the best stellar subset(s) for Oort constants measurement. Two, it enables us to characterize the deviations in *Gaia*'s observational result from the expected model. The larger significance of this work is to constrain a spatial range for future Oort constants analysis.

The recent third release of *Gaia* in December 2020 adds 200 million new samples to our database (Gaia Collaboration et al. 2020). This work also looks forward to using this very new measurement to derive Oort constants.

### ACKNOWLEDGMENTS

This work has made use of data from the European Space Agency (ESA) mission *Gaia* (<https://www.cosmos.esa.int/gaia>), processed by the *Gaia* Data Processing and Analysis Consortium (DPAC, <https://www.cosmos.esa.int/web/gaia/dpac/consortium>). Funding for the DPAC has been provided by national institutions, in particular the institutions participating in the *Gaia* Multilateral Agreement.

I would like to acknowledge the tremendous opportunity to do this work offered by Dr.Zhaoyu Li and Dr.Juntai Shen from Shanghai Jiaotong University, as well as Prof.Karen Masters, and their continuous supports throughout the project.

*Software:* Astropy (Astropy Collaboration et al. 2013, 2018), galpy (Bovy 2015), emcee (Foreman-Mackey et al. 2013) .

## REFERENCES

- Andrae, R., Fouesneau, M., Creevey, O., et al. 2018, A&A, 616, A8, doi: [10.1051/0004-6361/201732516](https://doi.org/10.1051/0004-6361/201732516)
- Astropy Collaboration, Robitaille, T. P., Tollerud, E. J., et al. 2013, A&A, 558, A33, doi: [10.1051/0004-6361/201322068](https://doi.org/10.1051/0004-6361/201322068)
- Astropy Collaboration, Price-Whelan, A. M., SipHocz, B. M., et al. 2018, aj, 156, 123, doi: [10.3847/1538-3881/aabc4f](https://doi.org/10.3847/1538-3881/aabc4f)
- Binney, J., & Merrifield, M. 1998, Galactic Astronomy
- Bovy, J. 2015, ApJS, 216, 29, doi: [10.1088/0067-0049/216/2/29](https://doi.org/10.1088/0067-0049/216/2/29)
- . 2017, MNRAS, 468, L63, doi: [10.1093/mnrasl/slx027](https://doi.org/10.1093/mnrasl/slx027)
- Eilers, A.-C., Hogg, D. W., Rix, H.-W., & Ness, M. K. 2019, ApJ, 871, 120, doi: [10.3847/1538-4357/aaf648](https://doi.org/10.3847/1538-4357/aaf648)
- Feast, M., & Whitelock, P. 1997, MNRAS, 291, 683, doi: [10.1093/mnras/291.4.683](https://doi.org/10.1093/mnras/291.4.683)
- Foreman-Mackey, D., Hogg, D. W., Lang, D., & Goodman, J. 2013, PASP, 125, 306, doi: [10.1086/670067](https://doi.org/10.1086/670067)
- Gaia Collaboration, Smart, R. L., Sarro, L. M., et al. 2020, arXiv e-prints, arXiv:2012.02061, <https://arxiv.org/abs/2012.02061>
- Joy, A. H. 1939, ApJ, 89, 356, doi: [10.1086/144060](https://doi.org/10.1086/144060)
- Kerr, F. J., & Lynden-Bell, D. 1986, MNRAS, 221, 1023, doi: [10.1093/mnras/221.4.1023](https://doi.org/10.1093/mnras/221.4.1023)
- Kuijken, K., & Tremaine, S. 1994, ApJ, 421, 178, doi: [10.1086/173635](https://doi.org/10.1086/173635)
- Levine, E. S., Heiles, C., & Blitz, L. 2008, ApJ, 679, 1288, doi: [10.1086/587444](https://doi.org/10.1086/587444)
- Li, C., Zhao, G., & Yang, C. 2019, ApJ, 872, 205, doi: [10.3847/1538-4357/ab0104](https://doi.org/10.3847/1538-4357/ab0104)
- Lin, C. C., Yuan, C., & Roberts, W. W., J. 1978, A&A, 69, 181
- Metzger, M. R., Caldwell, J. A. R., & Schechter, P. L. 1998, AJ, 115, 635, doi: [10.1086/300198](https://doi.org/10.1086/300198)
- Mignard, F. 2000, A&A, 354, 522
- Mihos, C. unknown year, The Solar Motionnbsp;, <http://burro.case.edu/Academics/Astr222/Galaxy/Kinematics/solarmotion.html>
- Minchev, I., & Quillen, A. C. 2007, MNRAS, 377, 1163, doi: [10.1111/j.1365-2966.2007.11661.x](https://doi.org/10.1111/j.1365-2966.2007.11661.x)
- Mróz, P., Udalski, A., Skowron, D. M., et al. 2019, ApJL, 870, L10, doi: [10.3847/2041-8213/aaf73f](https://doi.org/10.3847/2041-8213/aaf73f)
- Ogrodnikoff, K. 1932, ZA, 4, 190
- Olling, R. P., & Dehnen, W. 2003, ApJ, 599, 275, doi: [10.1086/379278](https://doi.org/10.1086/379278)
- Olling, R. P., & Merrifield, M. R. 1998, MNRAS, 297, 943, doi: [10.1046/j.1365-8711.1998.01577.x](https://doi.org/10.1046/j.1365-8711.1998.01577.x)
- Oort, J. H. 1927, BAN, 3, 275
- Sellwood, J. A., & Carlberg, R. G. 2014, ApJ, 785, 137, doi: [10.1088/0004-637X/785/2/137](https://doi.org/10.1088/0004-637X/785/2/137)
- Siebert, A., Famaey, B., Minchev, I., et al. 2011, MNRAS, 412, 2026, doi: [10.1111/j.1365-2966.2010.18037.x](https://doi.org/10.1111/j.1365-2966.2010.18037.x)
- Sofue, Y., & Rubin, V. 2001, ARA&A, 39, 137, doi: [10.1146/annurev.astro.39.1.137](https://doi.org/10.1146/annurev.astro.39.1.137)
- Wegg, C., Gerhard, O., & Bieth, M. 2019, MNRAS, 485, 3296, doi: [10.1093/mnras/stz572](https://doi.org/10.1093/mnras/stz572)